Thermochimica Acta 472 (2008) 50–54

Contents lists available at ScienceDirect

Thermochimica Acta

journal homepage: www.elsevier.com/locate/tca

Calibration and desmearing of a differential thermal analysis measurement signal – upon heating and cooling – in the high-temperature region

Wolfgang Baumann, Andreas Leineweber*, Eric Jan Mittemeijer

Max Planck Institute for Metals Research, Heisenbergstrasse 3, 70569 Stuttgart, Germany

ARTICLE INFO

Article history:
Received 12 February 2008
Received in revised form 13 March 2008
Accepted 22 March 2008
Available online 29 March 2008

Keywords:
DTA
Calibration
Desmearing
Curie point
Cobalt
High-temperature region

ABSTRACT

A previously reported calibration and desmearing method for a differential thermal analysis (DTA) apparatus applicable to heating and cooling was successfully modified to be used in the high-temperature region (up to 1570 K). The method requires knowledge of parameters, which have a physical meaning, of the heat-flux model appropriate for the DTA apparatus. Values for these physical parameters were determined by calibration. As calibration materials Mo (exhibiting a smooth variation of specific heat with temperature) and Co (non-monotonic change of specific heat upon the ferro- to paramagnetic transition and vice versa) were employed. Experimental measures to improve the reproducibility were presented.

1. Introduction

Differential thermal analyses (DTA) are often used to determine heats of reaction/transformation, and to investigate reaction/transformation kinetics quantitatively as function of the heating/cooling rate [1,2]. To this end the DTA facility used first has to be calibrated with respect to the values of the heat capacity and the temperature. Moreover, and in particular for the analysis of reaction/transformation kinetics, the measurement signal has to be desmeared, since the measurement signal is smeared due to thermal lag [3], which affects the peak position and the peak shape.

Usually the heat-capacity calibration of isochronal (i.e. applying a constant heating/cooling rate) DTA is performed by calculating the apparent molar heat capacity of a sample, as follows. The temperature difference of a piece of calibration material with a well-known heat capacity and a reference cell is measured and it is assumed that this temperature difference is proportional to the heat capacity of the calibration specimen. In this method the smearing of the measurement signal over time is neglected [3]; because of this the determined heat capacity is an "apparent" heat capacity. The effect of smearing plays a significant role when the heat capacity changes drastically with temperature as for example around the Curie temperature.

Common practice for the temperature calibration upon heating involves the melting of pure materials [4–6]. The determined melting temperatures are equated to the literature values and thereby temperature calibration has been performed. Note that temperature calibration has to be performed for each heating rate [7].

A standard technique to desmear a DTA measurement signal is to use a temperature filter with parameters which have no physical meaning [8–10]. Desmearing procedures which consider the mode of operation and the experimental setup of the apparatus are typically very complex and in addition they are only suitable for isochronal *heating* modes [3,11].

The present work is based on previous work by Kempen et al. [3], where a combined temperature and heat-capacity calibration and desmearing method was developed for DTA. The method is applicable to heating and cooling experiments. It is based on a heat-flux model of the DTA with parameters which are independent of the heating/cooling rate applied. This model was previously applied successfully up to maximally 1100 K [3] by employing, in particular, the ferro- to paramagnetic transition of iron for the determination of the model parameters. A ferro- to paramagnetic transition, occurring at the Curie temperature, T_C, is suitable for the combined calibration and desmearing method, because such a transition is non-monotonic (i.e. the heat capacity goes to infinity at the Curie temperature) and consequently strongly smeared. In the present work the model was further developed for application to higher temperatures of up to 1570 K, by using the ferro- to paramagnetic transition of cobalt ($T_C^{Co} = 1396$ K) instead of that

* Corresponding author. Tel.: +49 711 689 3365; fax: +49 711 689 3312.
E-mail address: a.leineweber@mf.mpg.de (A. Leineweber).

0040-6031/$ – see front matter © 2008 Elsevier B.V. All rights reserved.
doi:10.1016/j.tca.2008.03.016

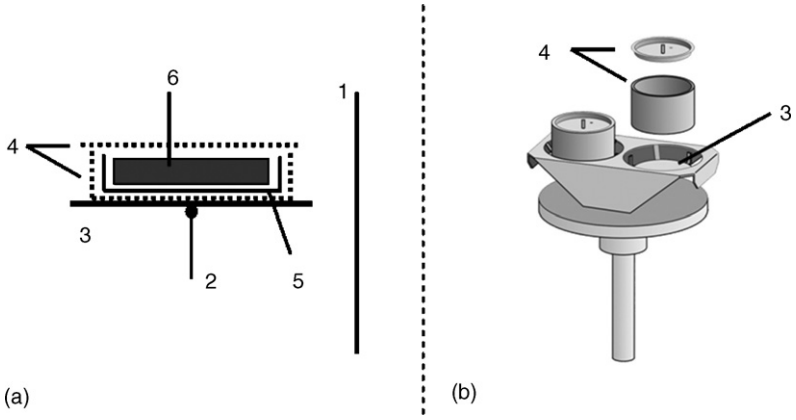

Fig. 1. (a) Schematic illustration of the sample measurement cell and its components redrawn after [3]; (b) schematic illustration of the measuring head [12]. (1) Furnace; (2) thermocouple; (3) pan holder/sample stage; (4) outer sample pan with lid; (5) inner sample pan; (6) sample.

of iron ($T_C^{Fe} = 1043$ K). Thereby, the quantitative investigation of reaction/transformation kinetics and the quantitative determination of heats of reaction/transformation have become possible in the high-temperature region.

2. Basis of the method

2.1. Heat flux model

A DTA apparatus measures the temperature difference between a sample and reference cell upon heating/cooling. The experimental setup of the sample measurement cell is shown in Fig. 1. The sample and the reference cells are identical and are placed symmetrically with respect to each other in the furnace; the reference cell is empty (see Fig. 1). From the furnace wall the heat is transported to the components of the sample measurement cell and the reference cell, and, depending on the heat capacities and the thermal resistances of the single components, heat transport also occurs between neighbouring components.

All components of the measurement cell are metallic (i.e. they have a small thermal resistance) except for the inner sample pan. The inner sample pan normally consists of inert, ceramic material (here Y_2O_3) to avoid chemical reactions between the outer sample pan (here Pt) and the sample at elevated temperatures.

The heat-transport characteristics of the sample measurement cell, s, and the reference cell, r, can be described using a heat-flux model of the DTA apparatus which consists of a limited number of heat resistances R and heat capacities C (cf. Fig. 2 in Ref. [3]). The heat, q, fluxes to the elements, t_r (thermocouple reference cell), r (reference cell), t_s (thermocouple sample cell) and s (sample measurement cell) (cf. Fig. 2 in Ref. [3]), can be described by the following equations [3]:

$$\frac{dq_{t,r}}{dt} = \frac{T_f - T_{t,r}}{R_t} - \frac{T_{t,r} - T_r}{R_s} = C_{p,t}\frac{dT_{t,r}}{dt} \quad (1)$$

$$\frac{dq_r}{dt} = \frac{T_{t,r} - T_r}{R_s} = C_{p,r}\frac{dT_r}{dt} \quad (2)$$

$$\frac{dq_{t,s}}{dt} = \frac{T_f - T_{t,s}}{R_t} - \frac{T_{t,s} - T_s}{R_s} = C_{p,t}\frac{dT_{t,s}}{dt} \quad (3)$$

$$\frac{dq_s}{dt} = \frac{T_{t,s} - T_s}{R_s} = (C_{p,s} + C_{p,r})\frac{dT_s}{dt} \quad (4)$$

where T_f denotes the temperature of the furnace wall. T_s and T_r are the temperatures of the sample cell, s, and the reference cell, r (cf. Fig. 2 in Ref. [3]), respectively. $T_{t,s}$ and $T_{t,r}$ denote the temperatures of the thermocouples of the sample cell, t_s, and reference cell, t_r, respectively. $C_{p,s}$, $C_{p,r}$ and $C_{p,t}$ are the heat capacities of the sample, of the reference cell and of the thermocouple and its direct surroundings; t is the time. The measured variables are the temperature of the thermocouple of the reference cell, $T_{t,r}$, and the temperature difference of the thermocouples of the reference cell and the sample cell: $\Delta T_{t,s} = T_{t,s} - T_{t,r}$. The identical thermocouples t_r and t_s are not calibrated for absolute temperature determination. Hence, a temperature deviation of the thermocouple t_r, ΔT_{tc}, which is taken temperature and heating rate independent, has to be incorporated in the analysis.

The DTA facility can thus be described by five heating-rate and cooling-rate independent physical parameters: (i) the heat resistance, R_t, between the furnace and the thermocouples; (ii) the heat capacity of the thermocouple and its direct surroundings, $C_{p,t}$; (iii) the heat capacity of the reference cell, $C_{p,r}$; (iv) the heat resistance between sample measurement/reference cell and thermocouple, R_s; and (v) the thermocouple temperature shift, ΔT_{tc} (cf. Fig. 2 in Ref. [3]).

According to Kempen et al. [3] these five DTA parameters can be determined by measuring two calibration materials with known C_p:

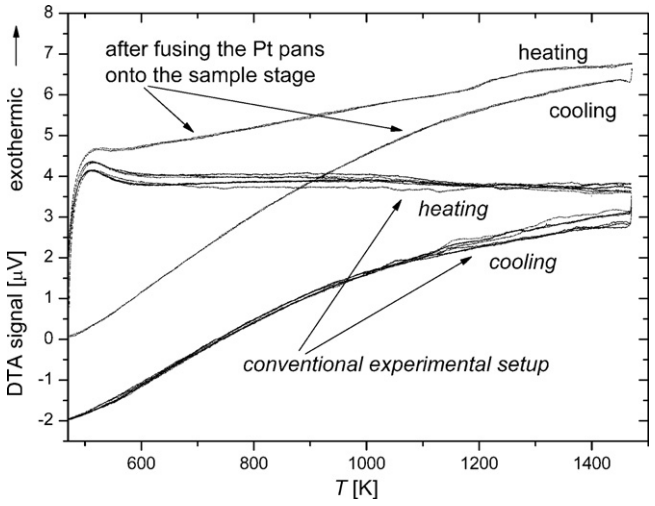

Fig. 2. Consecutive runs with empty sample measurement cell, recorded (i) with the conventional experimental setup (6 runs) and (ii) after the Pt pans had been fused onto the sample stage (2 runs); heating/cooling rate 10 K/min.

One material (a) should exhibit a heat capacity that varies smoothly with temperature, the other one (b) should show a strong, preferably non-monotonic, temperature dependence of the heat capacity. In Ref. [3] for (a) sapphire and for (b) iron with its ferro- to paramagnetic transition at $T_C^{Fe} = 1043\,K$ were used.

On the basis of the DTA data recorded from the calibration materials for various heating/cooling rates, the above-mentioned physical parameters describing the DTA apparatus can be determined. In order to extend the applicability of the method to high temperatures, in the present work molybdenum and cobalt were used as calibration materials (a) and (b), respectively. Cobalt has its ferro- to paramagnetic transition at $T_C^{Co} = 1396\,K$, which is about 353 K higher than the Curie temperature of iron T_C^{Fe}. The ferro- to paramagnetic transitions of iron and cobalt show no temperature hysteresis [13,14] (no mass transport involved), so that the Curie temperature is heating- and cooling-rate independent [15].

The determination of the instrumental DTA parameters was done on the basis of literature data for the temperature dependent molar heat capacity of molybdenum, $C_{p,Mo}$, (cf. Section 2.2) and for the Curie temperature of Co (cf. Section 2.3) as follows (for details of the fit procedure, see Ref. [3]). Using literature data for $C_{p,Mo}$ as well as the DTA data recorded from the Mo measurements, first the temperature dependent parameter R_t was calculated (for each heating and cooling rate). Next, applying Eqs. (3) and (4), the calculated (temperature dependent) parameter R_t (averaged over all heating/cooling rates) and the recorded DTA data from the Co measurements, the molar heat capacity of Co, $C_{p,Co}$, was calculated. This calculation of $C_{p,Co}$ is based on a complex fit procedure during which the fit parameters $C_{p,t}$, $C_{p,r}$ and R_s are varied according to a simplex procedure [16], such that the $C_{p,Co}$ curves for different heating/cooling rates coincide. Finally, ΔT_{tc} was calculated as the difference of the calculated value and the literature value of the Curie temperature of cobalt. The thus obtained model description of the DTA apparatus can be validated by comparing the desmeared molar heat capacity of cobalt, $C_{p,Co}$, as function of temperature with literature data (cf. Section 2.3).

2.2. C_p of molybdenum

Molybdenum has a molar heat capacity that changes smoothly, monotonically with temperature. Temperature dependent values for the molar heat capacity of molybdenum $C_{p,Mo}$ were adopted as given in Ref. [17]. The uncertainties in the heat-capacity values were estimated not to exceed ±1.0%. The discrete values for $C_{p,Mo}$ from Ref. [17] can be described by a continuous fifth-order polynomial. The difference between the data points and the polynomial curve does not exceed ±0.1% and consequently can be neglected. It thus was obtained:

$$C_{p,Mo} = A_0 + A_1 T + A_2 T^2 + A_3 T^3 + A_4 T^4 + A_5 T^5 \quad \text{for } 273.15\,K \le T \le 1750\,K \tag{5}$$

with $A_0 = 17.1694\,J\,mol^{-1}\,K^{-1}$, $A_1 = 0.03515\,J\,mol^{-1}\,K^{-2}$, $A_2 = -5.35826 \times 10^{-5}\,J\,mol^{-1}\,K^{-3}$, $A_3 = 4.40757 \times 10^{-8}\,J\,mol^{-1}\,K^{-4}$, $A_4 = -1.70917 \times 10^{-11}\,J\,mol^{-1}\,K^{-5}$, $A_5 = 2.64523 \times 10^{-15}\,J\,mol^{-1}\,K^{-6}$.

2.3. C_p of cobalt

A number of publications provide data for the molar heat capacity of Co, $C_{p,Co}$, and the Curie temperature of cobalt, T_C^{Co} [18–25]. The data for $C_{p,Co}$ adopted in this work correspond to those taken up in the SGTE database [18] and to those given by Fernández Guillermet [19] who made a critical evaluation of data for the thermodynamic properties of cobalt (cf. Section 4).

3. Experimental

As DTA apparatus a DSC 404C Pegasus from Netzsch (the same DTA as used in Ref. [3]) has been employed. The apparatus is equipped with a DSC C_p sensor (thermocouple type S) and a high temperature noble-metal furnace. The measurements were performed under a dynamic argon atmosphere (99.9999%; flow rate 50 ml/min).

3.1. Improvement of the reproducibility of the DTA signal

First, a series of test measurements was conducted using the conventional experimental setup shown in Fig. 1 (right). Here it is necessary to lift up both Pt pans from the sample stage after each measurement to avoid diffusion bonding with the sample stage (see Fig. 1). This lift up and the following putting down influences the reproducibility of the measurements, since the (thermal) contact between the sample stage and the Pt pans is changed and because the Pt pans cannot be placed exactly at the same position as before (see Fig. 2).

Therefore the Pt pans were diffusion bonded on the sample stage so that position and contact area do not change in a series of consecutive measurements. Thus, only a transfer of the inner sample pan is necessary for the exchange of samples in a series of measurements (see Fig. 1).

The fusing of the Pt pans with the sample stage was performed after placing the Pt pans exactly in the middle of the sample stage. Afterwards consecutive calibration DTA runs were performed with heating up to 1720 K; the calibration runs were repeated until the subsequent runs showed no deviations from the previous runs.

The improvement of the reproducibility of the measurements by diffusion bonding of the Pt pans is obvious from the results shown in Fig. 2. Without this modification of the measurement setup (i.e. the fusing of the Pt pans) the required reproducibility of the measurements for the calibration and desmearing procedure in the high-temperature region would not have been achieved.

3.2. DTA runs

For the DTA measurements disc shaped Co (purity 99.998%) and Mo (purity 99.95%) samples with a diameter of approx. 5 mm and a thickness of about 1.4 mm were cut from rods of the respective pure metals. Subsequently the samples were ground and polished to clean the surface of the samples. For the last polishing step a 3 μm diamond paste was used.

Three subsequent runs were performed for each heating/cooling rate applied (here: 10, 15 and 20 K/min):

I. empty measurement;
II. cobalt sample;
III. molybdenum sample.

For every heating/cooling rate a new cobalt or molybdenum sample was used. During the measurement the samples were unavoidably slightly oxidised at the surface. To ensure that this oxidation does not affect the DTA measurement signal, second runs were carried out for the cobalt and molybdenum measurements and the results were identical to the results of the first run.

If the sample cell and the reference cell would exhibit the truly same setup, the empty run should cause a zero signal; i.e. there should be no temperature difference between the sample measurement cell and the reference cell. However, in reality a small difference in the setups for sample measurement cell and reference cell occurs, and therefore the measurement signal of the empty run

was subtracted from the corresponding signals of the Co and Mo measurement runs.

For the inner sample pan (cf. no. 5 in Fig. 1) Y_2O_3 was selected because this material shows no reaction with the calibration materials. At the bottom the Y_2O_3 pans had a thickness of about 0.2 mm. Note that for all measurements the same pans were used.

4. Results and discussion

The apparent molar heat capacity of cobalt, $C_{p,\mathrm{Co}}^{\mathrm{app.}}$, as function of temperature can be calculated (cf. second paragraph of Section 1) on the basis of the DTA measurement signal recorded for Co, $\Delta T_{\mathrm{t,Co}}$, using the DTA measurement signal recorded for Mo (calibration material), $\Delta T_{\mathrm{t,Mo}}$, and the known heat capacity of Mo, $C_{p,\mathrm{Mo}}$ (cf. Section 2.2): $C_{p,\mathrm{Co}}^{\mathrm{app.}} = C_{p,\mathrm{Mo}}(\Delta T_{\mathrm{t,Co}}/\Delta T_{\mathrm{t,Mo}})$. Results are shown in Fig. 3.

The true heat capacity is independent of heating and cooling rate. However, the apparent molar heat capacity of Co, determined as described above, strongly depends on the heating/cooling rate; also the ferro- to paramagnetic transition temperature shows a heating/cooling-rate dependence (see Fig. 3). These heating-rate and cooling-rate dependencies are caused by smearing due to thermal lag. The often used, simple calibration procedure, that provides the basis for the results shown in Fig. 3, is inadequate.

Application of the present calibration and desmearing method based on the heat-flux model (Section 2.1) led to results for the molar heat capacity as function of temperature shown in Fig. 4. Evidently, the desmearing procedure leads to coincidence of the curves pertaining to the different heating and cooling rates and thus an apparent thermal hysteresis of the ferro- to paramagnetic transition does not occur, as it should be (see also Fig. 5). The small remaining differences between the various molar heat capacity curves are within the experimental accuracy of the DTA measurements.

The average of the molar heat capacity curves of Co, $C_{p,\mathrm{Co}}$, (calculated from the plots in Fig. 4) can be compared with corresponding literature data (cf. Section 2.3) in Fig. 5. It follows that the molar heat capacity curve determined in this work agrees very well with the literature data.

The values obtained for the instrumental DTA (fit) parameters $C_{p,\mathrm{t}}$, $C_{p,\mathrm{r}}$, R_{s} and ΔT_{tc} (as listed in Section 2.1 and determined as described immediately above) have been gathered in Table 1. The values determined for these physical parameters as determined by Kempen et al. [3], for the same DTA apparatus but using different calibration materials and pertaining to a different temperature range, have also been given in Table 1.

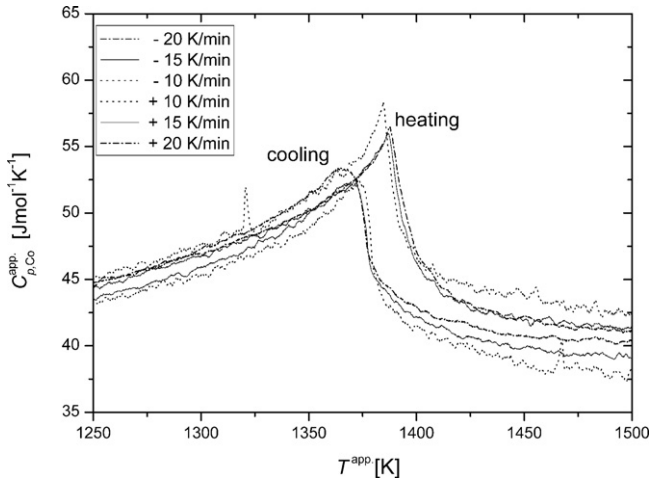

Fig. 3. Apparent molar heat capacity of Co, $C_{p,\mathrm{Co}}^{\mathrm{app.}}$, for three different heating and cooling rates; calculated as described at the beginning of Section 4.

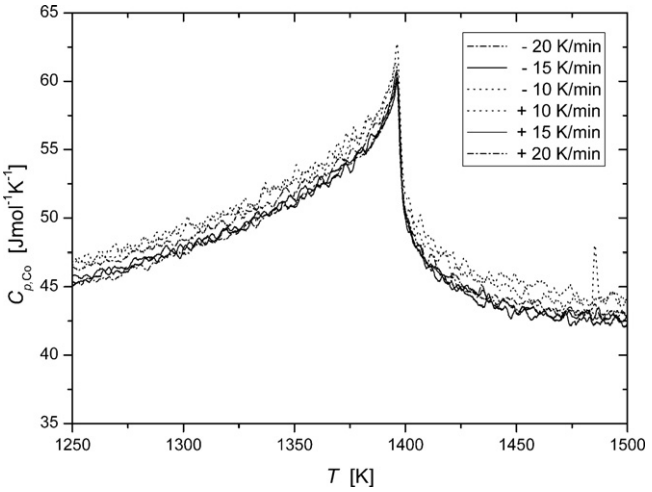

Fig. 4. Molar heat capacity of Co, $C_{p,\mathrm{Co}}$, for different heating/cooling rates after correction for thermal smearing according to the heat flux model.

The values determined here for $C_{p,\mathrm{t}}$ and $C_{p,\mathrm{r}}$ are of the same order of magnitude as those determined in Ref. [3]. The value for the heat resistance R_{s} (between sample and thermocouple) is one third smaller than the value determined in Ref. [3]. This can be understood as a consequence of (i) the fusing of the Pt-pan on the sample stage in the current work (so the thermal contact gets better) and (ii) the increasing contribution of radiation to heat transport with increasing temperature.

The increasing contribution of radiation to heat transport with increasing temperature also explains the decrease of the heat resis-

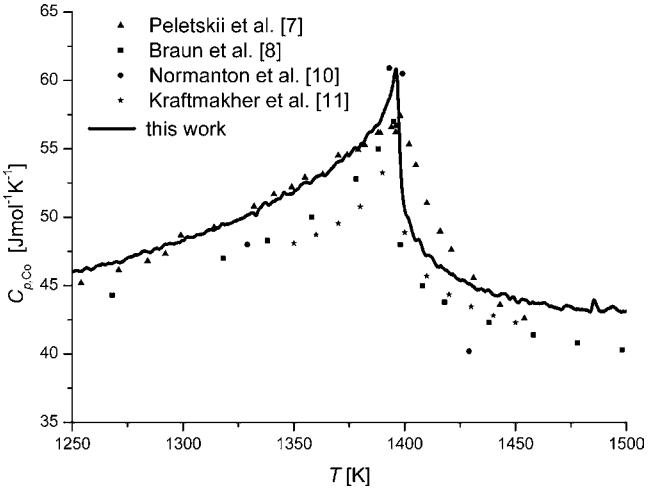

Fig. 5. Molar heat capacity of Co, $C_{p,\mathrm{Co}}$, (average calculated from the plots in Fig. 4) in comparison with literature data [20,21,23,24]. The literature data were shifted along the temperature axis such that the Curie temperatures coincide at $T_{\mathrm{C}}^{\mathrm{Co}} = 1396\,\mathrm{K}$ [18,19].

Table 1
Values for the instrumental DTA parameters as determined in this work in comparison with the values for these parameters determined in Ref. [3] for the same apparatus, but at a lower temperature range

	T range (K)	$C_{p,\mathrm{t}}$ (J/K)	$C_{p,\mathrm{r}}$ (J/K)	R_{s} (K s/J)	ΔT_{tc} (K)
This work	1250–1570	0.0500	0.0429	38.4520	15.2
Kempen et al. [3]	930–1110	0.0676	0.0326	61.2359	7.1

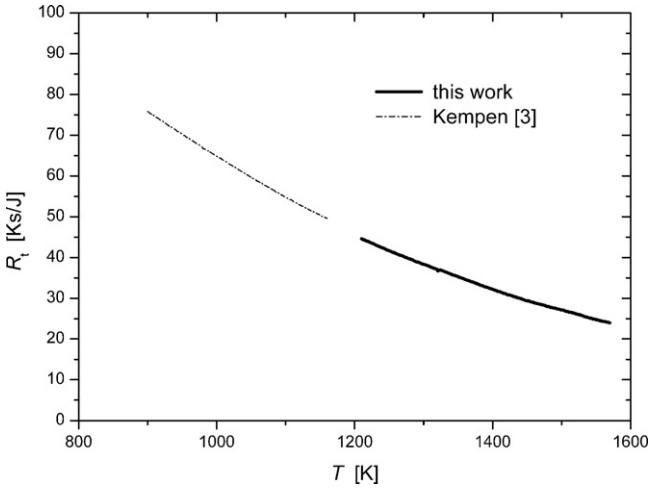

Fig. 6. The heat resistance R_t between the furnace wall and the thermocouples as a function of temperature.

tance R_t (between the furnace wall and the thermocouples) with increasing temperature (see Fig. 6). In particular, the dependence of R_t on temperature, for the temperature range investigated in Ref. [3] is, by extrapolation, very well compatible with the results obtained here at considerably higher temperatures.

5. Conclusions

- Calibration and desmearing of differential thermal analysis scans (temperature difference of sample and reference pans as function of temperature) – upon heating and cooling – is possible in the high-temperature region (up to, at least, 1570 K).
- By fusing of the (Pt) sample and reference pans on the sample stage the reproducibility of the measurements is improved considerably. Without this modification of the measurement setup the required reproducibility for the calibration and desmearing procedure in the high-temperature region cannot be achieved.
- The heat flux model, originally derived in Ref. [3], can be applied in a temperature region much larger than in the original work, recognising temperature dependence of the instrumental DTA parameters. Thereby the physical basis of the (fit) parameters of the model is corroborated.

Acknowledgements

This work was funded by the Max Planck Society within the inter-institutional research initiative “The Nature of Laves Phases”.

The authors thank Prof. Dr. F. Sommer for valuable discussion.

References

[1] G. Höhne, W. Hemminger, H.-J. Flammersheim, Differential Scanning Calorimetry, Springer-Verlag, Berlin, Heidelberg, 1996.
[2] F. Liu, F. Sommer, C. Bos, E.J. Mittemeijer, Int. Mater. Rev. 52 (2007) 193.
[3] A.T.W. Kempen, F. Sommer, E.J. Mittemeijer, Thermochim. Acta 383 (2002) 21.
[4] E. Gmelin, S.M. Sarge, Thermochim. Acta 347 (2000) 9.
[5] G.W.H. Höhne, H.K. Cammenga, W. Eysel, E. Gmelin, W. Hemminger, Thermochim. Acta 160 (1990) 1.
[6] H.K. Cammenga, W. Eysel, E. Gmelin, W. Hemminger, G. Höhne, S.M. Sarge, Thermochim. Acta 219 (1993) 333.
[7] J.D. Menczel, J. Therm. Anal. Cal. 49 (1997) 193.
[8] H.-J. Flammersheim, N. Eckardt, W. Kunze, Thermochim. Acta 187 (1991) 269.
[9] S. Wiesner, E. Woldt, Thermochim. Acta 187 (1991) 357.
[10] G.P. Krielaart, S. van der Zwaag, Mater. Sci. Technol. 14 (1998) 10.
[11] W. Poessnecker, Thermochim. Acta 187 (1991) 309.
[12] Netzsch, Instrument Manual Netzsch DSC 404C Pegasus, 1998.
[13] E. Kneller, Ferromagnetism, 1st edition, Springer, Berlin, 1962.
[14] R.M. Bozorth, Ferromagnetism, 2nd edition, D. van Nostrand Co., Toronto, 1951.
[15] Y.H. Jeong, D.J. Bae, I.K. Kwon, I.K. Moon, J. Appl. Phys. 70 (1991) 6166.
[16] W.H. Press, S.A. Teukolsky, W.T. Vetterling, B.P. Flannery, Numerical Recipes in C, Cambridge University Press, NY, 1997.
[17] J.P. Cali, (NIST Database 1977) Standard Reference Material 781.
[18] A.T. Dinsdale, Calphad 15 (1991) 317.
[19] A. Fernández Guillermet, Int. J. Thermophys. 8 (1987) 481.
[20] V.E. Peletskii, E.B. Zaretskii, High Temp.-High Press. 13 (1981) 661.
[21] M. Braun, R. Kohlhaas, Z. Naturforsch. A 19a (1964) 663.
[22] M. Braun, R. Kohlhaas, Phys. Status Solidi 12 (1965) 429.
[23] A.S. Normanton, Met. Sci. 9 (1975) 455.
[24] Y.A. Kraftmakher, T.Y. Romashina, Sov. Phys.-Sol. State 8 (1966) 1562.
[25] E.A. Owen, D. Madoc Jones, Proc. Phys. Soc. Lond. B 67 (1954) 456.